Hindawi
Mathematical Problems in Engineering
Volume 2019, Article ID 2719849, 14 pages
https://doi.org/10.1155/2019/2719849

Research Article

The Slashed-Rayleigh Fading Channel Distribution

E. Gómez-Déniz,[1] **L. Gómez**,[2] **and H. W. Gómez**[3]

[1]*Department of Quantitative Methods and TiDES Institute, University of Las Palmas de Gran Canaria, Spain*
[2]*Electronic Engineering and Automatic Department, University of Las Palmas de Gran Canaria, Spain*
[3]*Departamento de Matemáticas, Facultad de Ciencias Básicas, Universidad de Antofagasta, Chile*

Correspondence should be addressed to E. Gómez-Déniz; emilio.gomez-deniz@ulpgc.es

Received 21 November 2018; Accepted 14 January 2019; Published 11 February 2019

Academic Editor: Giovanni Falsone

We propose an alternative distribution for modelling fading-shadowing wireless channels. This distribution presents certain advantages over the Rayleigh-lognormal distribution and the K distribution and has proved useful in the setting described. We obtain closed-form expressions for the average channel capacity and for the average bit error rate of differential phase-shift keying and of minimum shift keying when the new distribution is used. This distribution can be obtained exactly as the sum of mutual independent Gaussian stochastic processes, because it must represent the simulation of the fading channel; that is, it simulates the signal envelope. Finally, we describe practical applications of this distribution, comparing it with the Rayleigh-lognormal and K distributions.

1. Introduction

Mobile communications systems must address various challenges that seriously degrade signal strength. A major problem in this respect is that of the fading signal, i.e., interference to the multiple scattered radio paths between the base station and the vicinity of the mobile receptor. When this occurs, the received signal exhibits rapid signal level fluctuations which are generally Rayleigh distributed.

The multipath channel resembles a physical communication channel and is characterised by bandwidth and gain. For the case of a mobile radio channel with constant gain and a linear phase response over the bandwidth that is greater than the bandwidth of the transmitted signal, the signal received at the terminal will undergo *flat fading*. This is the most common type of fading and the most widely studied (Rappaport [1]). In this situation, the strength of the received signal will oscillate rapidly due to multipath effects.

Figure 1 illustrates a simplified fading model between a stationary source (emitter) and a mobile vehicle (for a complete description of fading modelling, see Barts and Stutzman [2], Rappaport [1], Borhani et al. [3], and Lopez-Fernandez et al. [4]). Several components are involved; first, in the case of clear line of sight between the stationary source (emitter) and the mobile vehicle, no scattering mechanism is involved, although Doppler effects will be considered. However, a multipath or diffuse component (phase-incoherent wave) is created by the multiple (*random*) reflections (*scattering processes*) of the signal from scattered elements such as mountains and buildings. This component has little directivity and its magnitude is assumed to be Rayleigh distributed while its phase is uniformly distributed.

The specular component is a phase-coherent ground-reflected wave that is related to points close to where the receptor (i.e., the vehicle) is dynamically located. This component is responsible for strong fades, with an amplitude comparable to that of the direct component, although its phase is opposite Suh [5].

Figure 1 also shows the case of blocked line of sight between the stationary source and the mobile vehicle. In this case, the diffuse component is as before (and can be modelled by a Rayleigh distribution), but there is a new element, the shadowed direct component, produced by the scattering of the signal by the leaves, branches, and limbs of trees and by vegetation in general. In consequence, the signal is attenuated, to a degree that depends on the length of its path through the scattering element. The fading produced by this process is called fading-shadowing and can be modelled

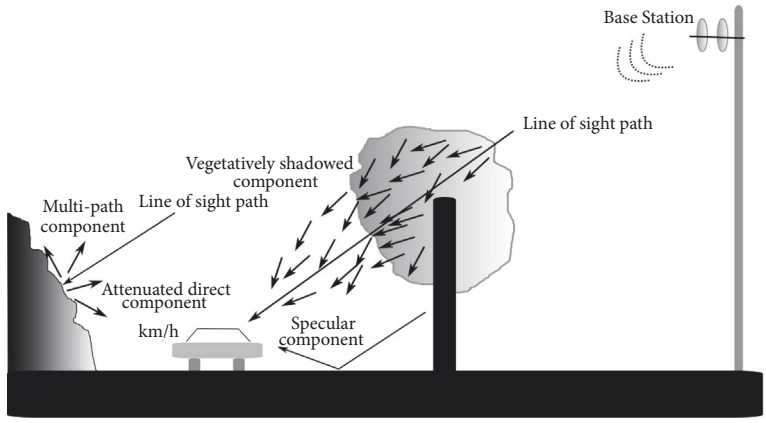

Figure 1: Illustration of fading components.

by the Rayleigh-lognormal (RLN) distribution (Hansen and Meno [6]), although this has a complicated integral form, or by the K distribution Abdi and Kaveh [7]. The latter distribution may be viewed as a Rayleigh distribution with a gamma distribution and it has a simpler form than the RLN.

This study examines fading-shadowing mechanisms in particular. However, as our proposal also contains the Rayleigh as a general case, it also applies to modelling the diffuse component.

To achieve a probability distribution that will efficiently model fading effects, a distribution should be expressed through simple mathematical expressions and subsume the Rayleigh distribution. Given this, parameter estimation is straightforward and second-order statistics such as fading descriptors (level crossing-rate (LCR), average fade duration (AFD), average bit error rate (BER), differential phase-shift keying (DFSK), and minimum shift keying (MSK)) can easily be computed (see, for instance, Proackis and Salehi [8], Adachi et al. [9], and Subbarayan [10], for a comprehensive description of these estimators).

The above conditions are met by the Slashed-Rayleigh (SR) distribution, a two-parameter distribution that was first proposed by Iriarte et al. [11]. However, the latter did not address the question of fading applications. As we discuss below, this distribution is well suited to modelling flat fading effects in wireless communications.

Among the benefits offered by the SR distribution, it includes the Rayleigh distribution, thus facilitating the physical modelling of multipath signal propagation through phasors (complex signal representation).

We complete the description of the SR distribution as follows. First, we simulate it by Monte Carlo analysis (i.e., taking a statistical approach). Then, as required for a fading distribution, we simulate the distribution from a summation of phasors while accounting for Doppler effects (i.e., a physical approach), by embedding the SR distribution within Clarkes's model Rappaport [1], which is known to be appropriate for flat fading.

Although fading effects are apparent in general for mobile communications, they are especially noticeable in moving vehicles, where the signal received commonly presents multipath components and not just the direct component. However, for a stationary receiver, too, if the surrounding objects are moving, Doppler shift on the multipath components will affect the quality of the transmitted signal. The models we discuss can be applied to both stationary and moving receptors.

The outline of this paper is as follows. The SR distribution is presented in Section 2. Section 3 then introduces the SR phasor, shows some simulation plots, and discusses specific mathematical measures for the new distribution, together with metrics related to modelling fading effects in wireless communication channels. In Section 4, the SR distribution is compared with other distributions that are commonly used to account for the statistics of mobile radio signals. The simulation of the SR distribution through Monte Carlo analysis and the physical modelling of the multipath fading channel are discussed in Section 5. Finally, the main conclusions drawn are summarised in Section 6.

2. The Slashed-Rayleigh Distribution

The Rayleigh fading model can be used to simulate the situation in which a radio signal is scattered before it arrives at the receiver due to the presence of multiple objects in the environment. According to the central limit theorem, given sufficient scatter, the channel impulse response will be well modelled as a Gaussian process irrespective of the distribution of the individual components. If there is no dominant component to the scatter, this process will have a zero mean and its phase will be uniformly distributed between 0 and 2π radians. Therefore, the envelope of the channel response will be Rayleigh distributed, with the following probability density function (pdf)

$$g(r;\alpha) = \frac{r}{\sigma}\exp\left\{-\frac{r^2}{2\sigma}\right\}, \quad r \geq 0,\ \sigma > 0, \tag{1}$$

where $E(R^2) = 2\sigma$ is the expected value of R^2. In this case we write $R \sim \mathrm{R}(\alpha)$.

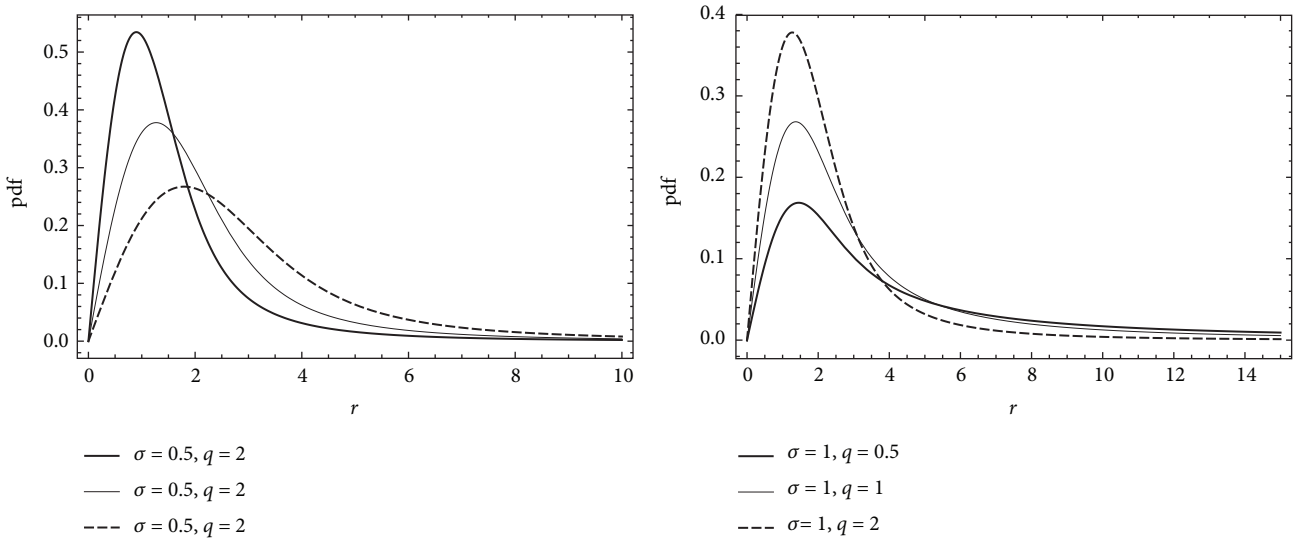

Figure 2: Illustration of the $SR(\sigma, q)$ distribution for a set of different parameter values.

As Tse ([12], p. 49) pointed out, *the model based on the Rayleigh fading is quite reasonable for scattering mechanisms when there are many small reflectors, but it is adopted primarily for its simplicity in typical cellular situations with a relatively small number of reflectors.* For this reason some alternatives to the Rayleigh fading model have been proposed, such as the RLN distribution with pdf, described by (Hansen and Meno [6] and Stuber [13])

$$f_X(x) = \int_0^\infty \frac{x}{\sigma} \frac{\exp\left(-x^2/(2\sigma)\right)}{\sigma\sqrt{2\pi\lambda^2}} \exp\left[\frac{-(\log\sigma-\mu)^2}{2\lambda^2}\right] dy, \quad x>0,\ \lambda>0,\ \mu\in\mathbb{R}. \tag{2}$$

The K distribution (Abdi and Kaveh [7]), obtained by compounding a Rayleigh distribution with a gamma distribution, is similar to the RLN distribution but it has a simpler structure and its pdf admits a closed form, although due to the Bessel function the estimates of the parameters are not direct. Its pdf is given by

$$f_X(x) = \frac{2}{\alpha\Gamma(\beta+1)}\left(\frac{x}{2\alpha}\right)^{\beta+1} K_\beta\left(\frac{x}{\alpha}\right), \quad x\geq 0,\ \alpha>0,\ \beta>-1, \tag{3}$$

where $K_\nu(z)$ denotes the modified Bessel function of the second kind of order ν and argument z and which has a complicated integral form. The main advantage of this special function is that it is included in most of the statistical software currently available, such as R, Matlab, and Mathematica (see Ruskeepaa [14]). Apart from the RLN distribution, other alternatives based on the lognormal distribution include the Rayleigh-inverse Gaussian (RIG) distribution (Karmeshu [15]) which is subject to the same restriction as the above distribution and the generalisation of the Rayleigh distribution that was recently proposed by Gómez-Déniz and Gómez [16], which overcomes some of the disadvantages of the above distributions.

The SR distribution, proposed by Iriarte et al. [11], has the following pdf:

$$f_R(r;\sigma,q) = \frac{q(2\sigma)^{q/2}}{r^{q+1}}\Gamma\left(1+\frac{q}{2}\right)F\left(\frac{r^2}{2\sigma}, 1+\frac{q}{2}\right), \tag{4}$$

where $\sigma>0$, $q>0$, and $F(a,b) = (1/\Gamma(a))\int_0^b t^{a-1}\exp(-t)dt$ is the cumulative distribution function of the gamma distribution. Observe that the pdf given in (1) is obtained from (4) when q tends to ∞. Furthermore, this distribution tends to the Dirac delta function at 0 when σ tends to infinity. Henceforth, when a random variable R follows this distribution it will be represented as $R\sim SR(\sigma,q)$.

If $R\sim SR(\sigma,q)$ with scale parameter σ and kurtosis parameter q, then (4) can be represented as

$$SR(\sigma,q) = \frac{R(\sigma)}{U^{1/q}}, \tag{5}$$

where $R(\sigma)$ and $U(0,1)$ (the uniform distribution) are independent and $q>0$.

Using the following expression, which relates the incomplete gamma function with the Kummer confluent hypergeometric function

$$\Gamma(a,z) = \Gamma(a) - \frac{z^a}{a}\,{}_1F_1(a,a+1,-z), \tag{6}$$

the pdf given in (4) can be rewritten as

$$f_R(r;\sigma,q) = \frac{qr}{\sigma(q+2)}\,{}_1F_1\left(\frac{q}{2}+1;\frac{q}{2}+2;-\frac{r^2}{2\sigma}\right). \tag{7}$$

Now, from (7) and using Kummer's first theorem we have

$$f_R(r;\sigma,q) = \frac{qr\exp\left(-r^2/(2\sigma)\right)}{\sigma(q+2)}\,{}_1F_1\left(1;\frac{q}{2}+2;\frac{r^2}{2\sigma}\right). \tag{8}$$

Figure 2 shows slopes of the pdf of the $SR(\sigma,q)$ distribution, revealing the dependency of the scale parameter σ and the shape parameters q (the fading).

2.1. Additional Features. The cumulative distribution function of $R(\sigma, q)$ is given by

$$\begin{aligned} F_R(r;\sigma,q) &= P(R \le r) \\ &= 1 - \exp\left(-\frac{r^2}{2\sigma}\right) \\ &\quad - \left(\frac{2\sigma}{r^2}\right)^{q/2} \Gamma\left(1+\frac{q}{2}\right) F\left(\frac{r^2}{2\sigma}, 1+\frac{q}{2}\right), \end{aligned} \tag{9}$$

which can be used to obtain the hazard function of the random variable $R \sim SR(\sigma, q)$, given by

$$\begin{aligned} &h(r) \\ &= \frac{q}{r\left[r^q \Gamma(1+q/2)\, F\left(r^2/2\sigma, 1+q/2\right)\right] \exp\left(-r^2/2\sigma\right) + 1}. \end{aligned} \tag{10}$$

Let $R \sim SR(\sigma, q)$. Then, for $k = 1, 2, \ldots$ and $q > k$, it follows that the r-th moment of the proposed distribution is given by

$$E\left(R^k\right) = \frac{(2\sigma)^{k/2} q}{q-k} \Gamma\left(1+\frac{k}{2}\right). \tag{11}$$

Therefore, from (11) we obtain the mean and the variance of the distribution, which are given by

$$\begin{aligned} E(R) &= \frac{q}{q-1}\sqrt{\frac{\pi\sigma}{2}}, \quad q > 1, \\ \operatorname{var}(R) &= \frac{\sigma q\left[4(q-1)^2 - \pi q(q-2)\right]}{2(q-1)^2(q-2)}, \quad q > 2, \end{aligned} \tag{12}$$

respectively. Moment and maximum likelihood estimation is studied in detail in Iriarte et al. [11], where a simulation study is also performed.

The pdf of the SR distribution can be written as an infinite convex sum of Nakagami distributions. To do so, observe that from the series expansion of the Kummer confluent hypergeometric function in (8) this pdf can be rewritten as

$$\begin{aligned} &f_R(r) \\ &= \frac{q}{\sigma(q+2)} \sum_{k=0}^{\infty} \frac{\Gamma(q/2+2)}{\Gamma(q/2+2+k)} \frac{r^{2k+1}}{(2\sigma)^k} \exp\left(-\frac{r^2}{2\sigma}\right). \end{aligned} \tag{13}$$

Now, by performing on (13) the change of variable $r = z\sqrt{m}$, where $m \in \mathbb{N}^*$ and taking $k+1 = m$, (13) can be written as

$$\begin{aligned} &f_R(r) \\ &= \frac{q\Gamma(q/2+2)}{q+2} \sum_{m=1}^{\infty} \frac{\Gamma(m)}{\Gamma(q/2+m+1)} f_Z(z;\Omega,m), \end{aligned} \tag{14}$$

where

$$f_Z(z;\Omega,m) = \frac{2m^m z^{2m-1}}{\Gamma(m)\,\Omega^m} \exp\left(-\frac{mz^2}{\Omega}\right), \tag{15}$$

which is the Nakagami distribution with parameters $m \in \mathbb{N}^*$ and $\Omega = 2\sigma > 0$. Hence

$$\sum_{m=1}^{\infty} \frac{\Gamma(m)}{\Gamma(q/2+m+1)} = \frac{q+2}{q\Gamma(q/2+2)}. \tag{16}$$

Thus, we conclude that the SR distribution studied here can be written as an infinite convex sum of Nakagami distributions.

3. The Slashed Channel Rayleigh Phasor

In this section, we demonstrate that the SR distribution can be obtained in an exact form as the sum of mutual independent Gaussian stochastic processes, as is required in order to simulate the fading channel, i.e., the signal envelope.

It is known that Rayleigh fading envelopes can be generated from zero-mean complex Gaussian random variables. Other fading distributions (see, for instance, Yacoub et al. [17] for the Nakagami-m case) and the generalised Rayleigh distribution in Gómez-Déniz and Gémez [16] are obtained in a similar manner after some mathematical considerations. Hence, in line with these precedents, we must now prove that the phase and the amplitude of a given propagating signal are distributed according to a uniform pdf in the $[0, 2\pi]$ interval and the SR distribution, respectively.

Following Beckmann ([18], p. 118), consider the sum

$$S = Re^{i\theta} = \sum_{i=1}^{n} A_j e^{i\Phi_j} = (X, Y) = (R\cos\theta, R\sin\theta), \tag{17}$$

where $i = \sqrt{-1}$, the terms X (the in-phase phasor) and Y (quadrature phasor) are independent uniformly distributed phasors (UDP), and the A_j are all distributed identically. When n is large, and assuming that A_j is not correlated with the Φ_j, both X and Y will be distributed normally with mean 0 and variance $(1/2)n = \sum_{j=1}^{n} A_j^2$. Goldsmith [19], see page 69, pointed out that under some conditions this is also true for small n. Now, let $(1/2)n = \sum_{j=1}^{n} A_j^2 = \sigma U^{-2/q}$, where U represents the uniform distribution in $(0, 1)$. Then, the joint distribution of X and Y is

$$\pi(x, y) = \frac{u^{2/q}}{2\pi\sigma} \exp\left\{-\frac{\left(x^2+y^2\right)u^{2/q}}{2\sigma}\right\}. \tag{18}$$

Then, expressing (18) as polar coordinates

$$\begin{aligned} \pi(r,\theta) &= \frac{ru^{2/q}}{2\sigma\pi} \exp\left\{-\frac{r^2u^{2/q}}{2\sigma}\right\}, \\ &\qquad 0 \le \theta \le 2\pi, \ r \ge 0. \end{aligned} \tag{19}$$

In the following, we obtain the phase and the amplitude distributions.

Proposition 1. *The SR distribution satisfies the following:*

(i) *The phase distribution is uniform, i.e.,* $\pi(\theta) = 1/2\pi$, $0 \le \theta \le 2\pi$.

(ii) *The amplitude distribution is given by (4).*

Proof. From (19) it is straightforward to obtain the conditional distributions of θ and r given $U = u$, which are given by

$$\pi(\theta \mid u) = \int_0^{\infty} \pi(r,\theta)\, dr = \frac{1}{2\pi},$$
$$\pi(r \mid u) = \int_0^{2\pi} \pi(r,\theta)\, d\theta = \frac{ru^{2/q}}{\sigma} \exp\left\{-\frac{r^2u^{2/q}}{2\sigma}\right\}. \tag{20}$$

Then, the unconditional distribution (independent of u) for the phase is

$$\pi(\theta) = \int_0^1 \pi(\theta \mid u)\, du = \frac{1}{2\pi}, \quad 0 \le \theta \le 2\pi. \tag{21}$$

The unconditional distribution for the amplitude is given by

$$\pi(r) = \int_0^1 \frac{ru^{2/q}}{\sigma} \exp\left(-\frac{r^2}{2\sigma}u^{2/q}\right) du. \tag{22}$$

Now, in (22) we perform the change of variable $t = (r^2/2\sigma)u^{2/q}$ and obtain

$$\pi(r) = \frac{q(2\sigma)^{q/2}}{r^{q+1}} \int_0^{r^2/(2\sigma)} t^{q/2} \exp(-t)\, dt. \tag{23}$$

Hence, the result follows after identifying a gamma distribution within the integral. □

According to result (ii) in Proposition 1, if $R \mid U = u \sim R(\sigma u^{-2/q})$ and $U \sim U(0,1)$, then $R \sim SR(\sigma, q)$, i.e., pdf (4) can be represented as a scale mixture (compound) of the Rayleigh distribution and the uniform distribution on the unit interval. Moreover, this representation of the distribution facilitates parameter estimation via the expectation-maximisation (EM) algorithm.

3.1. Measures of Interest in the Fading Channel. The SR distribution can readily be obtained as a scale mixture of the Rayleigh distribution and the uniform distribution, which facilitates the computation of some measures of interest in the framework of the fading channel, such as the amount of fading (AF) (also known as the strength of intensity fluctuations), and the BER for DPSK and MSK when the SR distribution is employed as that of the fading channel.

First, in (8) we perform the change of variable $R^2 = Z$ to obtain

$$f_Z(z;\sigma,q) = \frac{q\exp(-z/(2\sigma))}{2\sigma(q+2)}\, {}_1F_1\left(1; \frac{q}{2}+2; \frac{z}{2\sigma}\right), \tag{24}$$

which is a generalisation of the exponential distribution proposed in Bhattacharya [20]. Thus, when $R \sim SR(\sigma, q)$, the received signal power is distributed according to (24) with mean $E(Z) = 2q\sigma/(q-2)$.

For a single-input/single-output system, the amount of fading (see Abdi and Kaveh [21]), given by $AF = \mathrm{var}(R^2)/E^2(R^2)$ for the $SR(\sigma, q)$ distribution proposed here is given by

$$AF = \frac{4\sigma(q-2)}{q-4} - 1, \quad q > 4, \tag{25}$$

which varies in the interval $(4\sigma - 1, \infty)$. We recall that the value of AF for the Rayleigh, $R(\sigma)$, distribution is $4\sigma - 1$.

It is well known (see Abdi and Kaveh [7]) that, for the standard Rayleigh, $R(\sigma u^{-2/q})$, the BERs for DPSK and MSK are given by

$$P_{b,DPSK} = \frac{1}{2(1+2\gamma\sigma u^{-2/q})},$$
$$P_{b,MSK} = \frac{1}{2}\left[1 - \sqrt{\frac{2\gamma\sigma u^{-}2/q}{1+2\gamma\sigma u^{-2/q}}}\right]. \tag{26}$$

Now, from (ii) in Proposition 1 we obtain, by compounding, the corresponding average BERs of DPSK and MSK for the SR distribution, as follows.

Proposition 2. *The average BERs of DPSK and MSK for the SR distribution are given by*

$$\overline{P}_{b,DPSK} = \frac{q}{4\gamma\sigma(2+q)}\, {}_2F_1\left(1, 1+\frac{q}{2}; 2+\frac{q}{2}; -\frac{1}{2\gamma\sigma}\right),$$
$$\overline{P}_{b,MSK} = \frac{1}{2}\left[1 - {}_2F_1\left(\frac{1}{2}, \frac{q}{2}; 1+\frac{q}{2}; -\frac{1}{2\gamma\sigma}\right)\right], \tag{27}$$

respectively. Here $\gamma = E_B/N_0$, where E_b is the transmitted energy per bit and N_0 is the noise power spectral density and

$${}_2F_1(a,b;c,z) = \frac{\Gamma(c)}{\Gamma(b)\Gamma(b-c)} \int_0^1 t^{b-1}(1-t)^{c-b-1}(1-tz)^{-a}\, dt \tag{28}$$

is the hypergeometric function.

Proof. By applying the composite rule we obtain

$$\overline{P}_{b,DPSK} = \int_0^1 P_{b,DPSK} du = \frac{1}{2}\int_0^1 \frac{u^{2/q}}{2\gamma\sigma + u^{2/q}} du. \tag{29}$$

Now, with the change of variable $z = u^{2/q}$ expression (29) reduces to

$$\overline{P}_{b,DPSK} = \frac{q}{8\gamma\sigma} \int_0^1 z^{q/2} \left(1 + \frac{z}{2\gamma\sigma}\right)^{-1} dz, \tag{30}$$

which is immediately identified with (28) after simple algebraic manipulation. The expression for $\overline{P}_{b,MSK}$ is obtained in a similar way. □

The average channel capacity for fading channel is a useful metric, in that it provides an estimation of the information

rate that the channel can support, with little probability of error. Channel capacity, C (see, for instance, Li et al. [22] Singh and Rawat [23], among others), is defined as

$$C = B\int_0^\infty \log_2(1+r)\, f_R(r)\, dr, \tag{31}$$

where B is the received signal bandwidth. Following Li et al. [22] the Shannon capacity of the Rayleigh fading channel is given by

$$C_R = B\exp\left(\frac{1}{2d\sigma}\right)E_1\left(\frac{1}{2d\sigma}\right), \tag{32}$$

where $E_n(x) = \int_1^\infty \exp(-xt)/t\, dt$, $d = S/(N_0B)$, S is the average transmit power receiving bandwidth B, and the mean channel gain is $\sqrt{\sigma\pi/2}$.

Proposition 3. *The average Shannon capacity of the SR fading channel is given by*

$$C_{SR} = Bq\left(\mathcal{H}_1 + \mathcal{H}_2 + \mathcal{H}_3\right), \tag{33}$$

where

$$\begin{aligned}
\mathcal{H}_1 &= -\frac{\gamma}{q}\,{}_1F_1\left(\frac{q}{2}, \frac{q}{2}+1, \frac{1}{2d\sigma}\right),\\
\mathcal{H}_2 &= \sum_{k=0}^{\infty}\frac{2\left[1+(q+k)\log 2\right]+(2k+1)\log(dq)}{k!\,(2k+q)^2},\\
\mathcal{H}_3 &= \sum_{j=1}^{\infty}\frac{(-1)^j}{jj!}\frac{1}{(d\sigma)^j(q+2j)}
\end{aligned} \tag{34}$$

and $\gamma \approx 0.577216$ *is Euler's constant.*

Proof. Again, from the composite rule and using (32) with $\sigma \equiv \sigma u^{-2/q}$ we obtain

$$C_{SR} = B\int_0^1 \exp\left(\frac{u^{2/q}}{2d\sigma}\right)E_1\left(\frac{u^{2/q}}{2d\sigma}\right)du. \tag{35}$$

It is known (see Gautschi et al. [24] and Lin et al. [25]) that

$$E_1(z) = -\gamma - \log z + \sum_{j=1}^{\infty}(-1)^j\frac{z^j}{jj!}. \tag{36}$$

Thus, we have

$$\begin{aligned}
C_{SR} = B\int_0^1 &\exp\left(\frac{u^{2/q}}{2d\sigma}\right)\\
&\cdot\left[-\gamma - \log\left(\frac{u^{2/q}}{2d\sigma}\right) + \sum_{j=1}^{\infty}\frac{(-1)^j}{jj!}\left(\frac{u^{2/q}}{2d\sigma}\right)^j\right]du,
\end{aligned} \tag{37}$$

from which the result follows, after some algebraic manipulation. □

Table 1: Parameter values for the RLN, K, and SR distributions.

		Setting		
Model	Parameters	A	B	C
RLN	μ	0.63	0.51	–1.57
	λ	0.85	1.21	1.56
K	α	1.00	1.00	1.00
	β	0.35	–0.37	–0.65
SR	σ	1.14	0.36	0.14
	q	3.45	2.80	2.50

4. Comparisons

Figure 3 shows the average BERs for DPSK and MSK for the RLN, K, and SR distributions, for the three sets of parameter values given in Table 1. The BERs for the RLN and RIG distributions were computed numerically for DPSK and MSK using the same parameter values for the K distribution as in Abdi and Kaveh [21], in three settings: Setting A for $\beta = 0.35$, Setting B for $\beta = -0.37$, and Setting C for $\beta = -0.65$. In every case $\alpha = 1$. The corresponding parameter values for the RLN and SR distributions were computed by equating the population moments to the moments of the K distribution obtained using the above values of (α, β). We recall that the population moments of the K distribution are given by $E(R^k) = (2\alpha^k)\Gamma(1+k(2)\Gamma(1+\beta+k/2)/\Gamma(\beta+1)$, $k = 1, 2, \ldots$, while the first and second moments of the RLN distribution are $E(R) = \sqrt{\pi/2}\exp[(1/8)(\lambda^2+4\mu)]$ and $E(R^2) = 2\exp(\lambda^2/2+\mu)$, respectively. The moments of the SR distribution are given in (11). The estimated parameter values of the RLN distribution, λ and μ, differ from those obtained by Abdi and Kaveh [21] because the latter study used the approximation given in Abdi and Kaveh [7].

The graphs show that the SR distribution is a valuable means of predicting the BER in multipath dispersion fades. Compared with the K distribution, SR also achieves a good fit with the RLN distribution. The third scenario is conclusive in this case. We recall that the RLN distribution is commonly used in DPSK and MSK modulation schemes. It should also be noted that, for the RLN distribution, there is no closed-form expression for the average BER, which must be calculated by numerical integration methods (generally, the Gauss-Hermite method). Cygan [26] proposed an exact but complicated formula for estimating the BER in the DPSK case when the RLN distribution is used.

The analytical expressions of the SR and K distributions both include special functions, namely, the incomplete gamma function and the modified Bessel function, respectively. The two are similar and either can be used as a substitute for the RLN distribution. Therefore, the proposed distribution can be applied efficiently to capture the bleached shading aspects of the wireless channels.

Figure 4 shows the pdf of the RLN, K and SR distributions for the parameters given in Settings A, B, and C. Note that the SR distribution presents a longer tail than the other distributions.

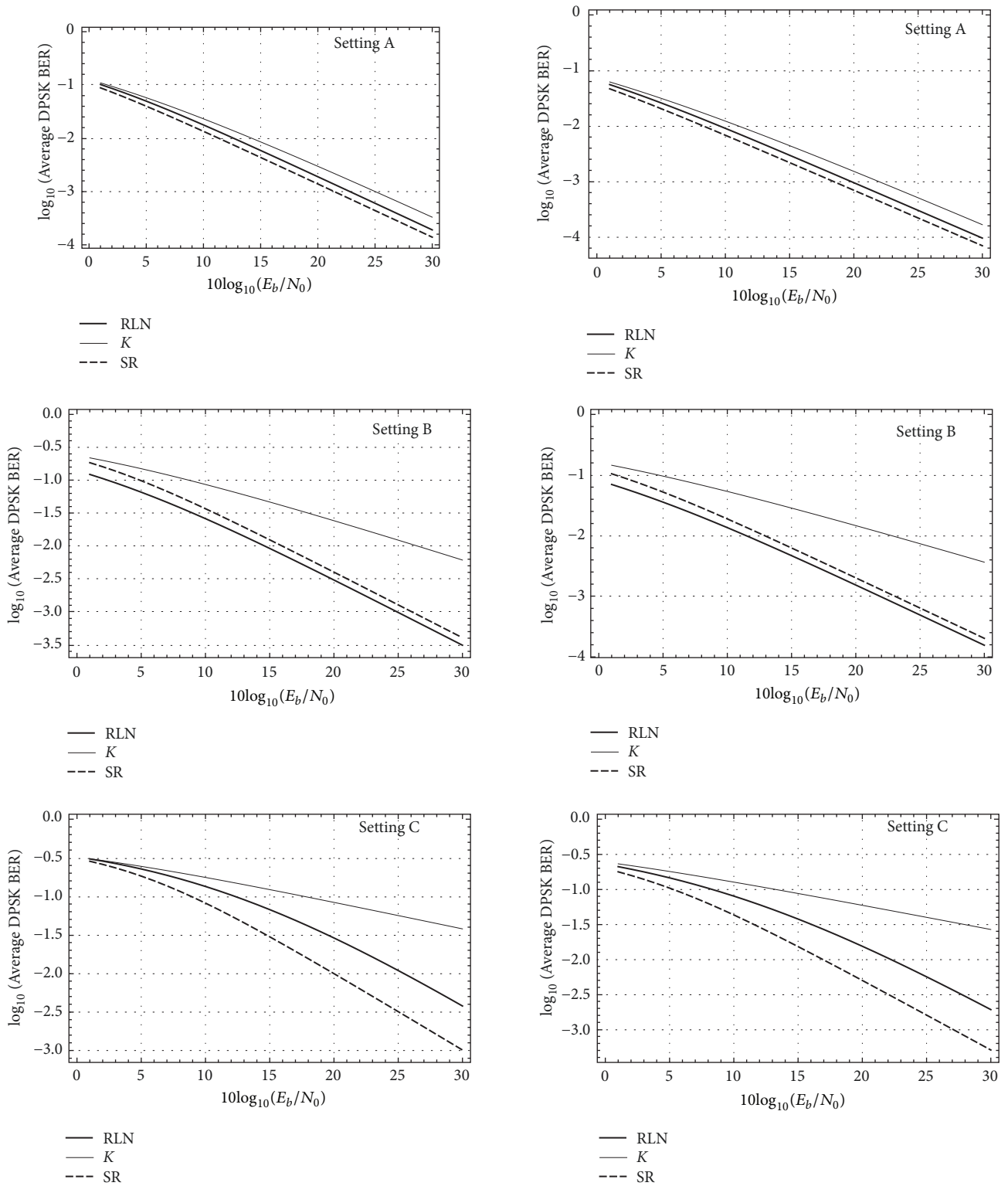

Figure 3: Average BERs of DPSK and MSK for the RLN, K, and SR distributions assuming the parameter values, for different settings, given in Table 1.

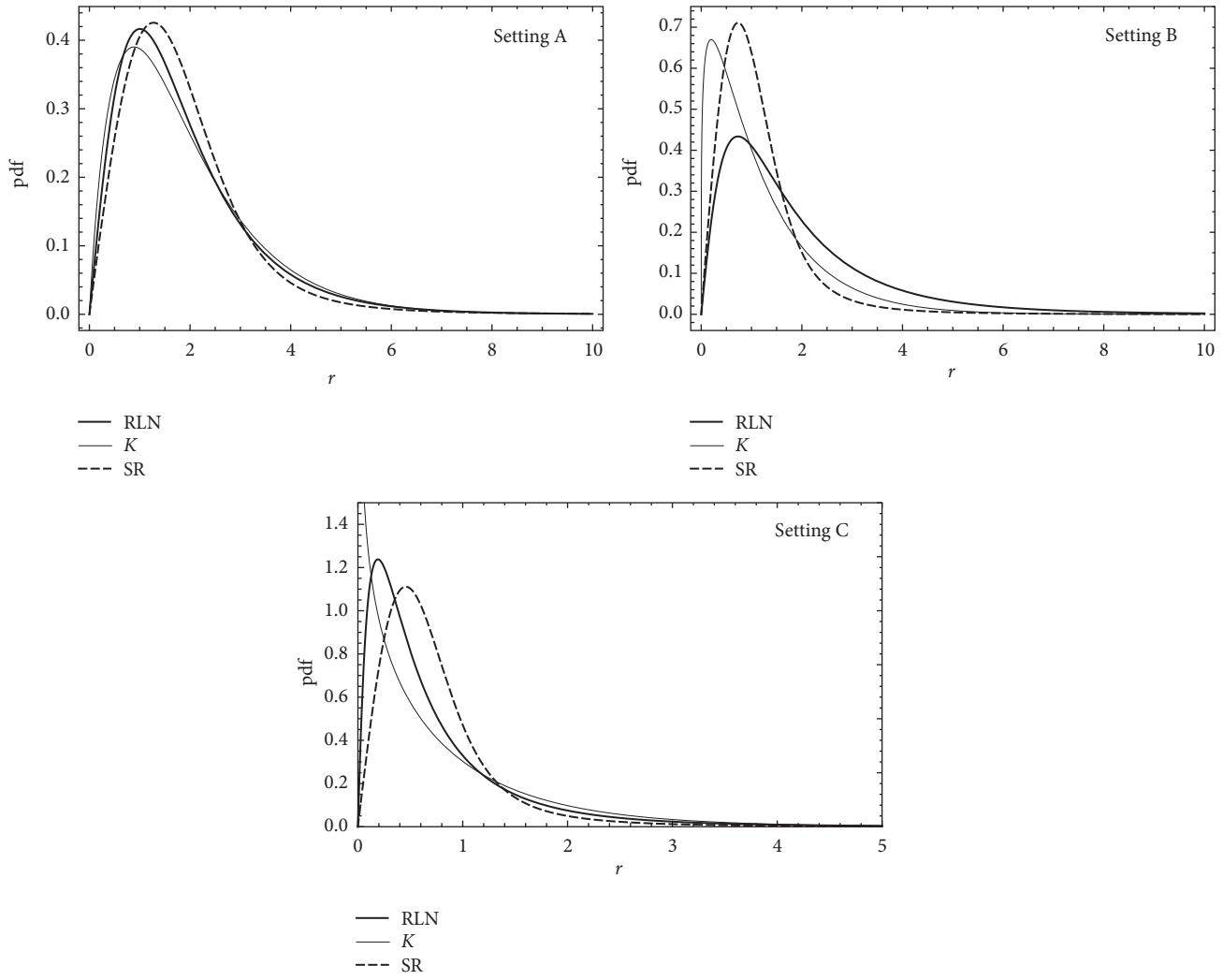

Figure 4: Slopes of the pdf for the RLN, K, and SR distributions for the parameters given in Settings A, B, and C.

4.1. Comparison with the RL and K Distributions. The distance or relative information between two probability distributions can be determined by the Kullback-Leibler divergence measure (see Hall [27], among others), which is defined as follows. Let f and g be probability densities on $\mathbb{R}^n$ such that f is absolutely continuous with respect to g (that is, $g(x) = 0$ implies $f(x) = 0$), and then the relative information or Kullback-Leibler divergence, $D_{KL}(f \parallel g)$ of f with respect to g, is

$$D_{KL}(f \parallel g) = \int_0^\infty f(x) \log\left[\frac{f(x)}{g(x)}\right] dx, \tag{38}$$

with the convention that $0/0 = 1$. When f is not absolutely continuous with respect to g we define $D_{KL}(f \parallel g) = \infty$. A disadvantage of (38) is that the Kullback-Leibler divergence is not symmetric and therefore is not a genuine distance metric. To overcome this problem, we use the Jensen-Shanon divergence (see, for instance, Lin [28]) given by

$$D_{JSD}(f \parallel g) = \frac{1}{2}\left(D_{KL}(f \parallel m) + D_{KL}(g \parallel m)\right), \tag{39}$$

where $m = (f + g)/2$. The integrated squared error (ISE) (Bowman [29]) is given by

$$D_{ISE}(f \parallel g) = \int_0^\infty \left(f(x) - g(x)\right)^2 dx. \tag{40}$$

Table 2 shows the Jensen-Shannon divergence for the K and SR distributions. Here, we see that, except for Setting A, the SR distribution presents the least distance with respect to the RL distribution, which was taken as the reference distribution.

5. Simulating the Proposed Distribution

To properly model a fading process, a random variate must be generated according to the proposed density distribution. Moreover, the random variate must be generated at low computational cost.

To achieve this, we proceed as in Gómez-Déniz and Gómez [16], using the well-known inverse transform method. Although there exist a plethora of methods for simulating

Input:
Alpha: α parameter ($\alpha \in \mathbb{R}$)
Q: q parameter ($q \in \mathbb{R}$)
A: range of data (Amplitude $\in \mathbb{R}$)
NSamples: number of samples (NSamples $\in \mathbb{N}$)
Output:
Z: set of data ~ $SR(\alpha, q)$
Begin:
v $\longleftarrow$ CDF(Alpha, Q) (0 $\longrightarrow$ A) ▷ *Obtain the CDF and store it within a vector*
for $i \longleftarrow 1$ *to NSamples* **do**
u $\longleftarrow$ rand ▷ *Obtain a uniform random sample*
$Z(i) \longleftarrow \max\{v \leq u\}$
end for
End

Algorithm 1: Simulating the SR distribution.

Table 2: Numerical values of the JSD and ISE measures for the K and SR distributions in comparison with the RLN distribution.

		Setting		
Measure	Model	A	B	C
JSD	K	0.0013	0.0499	0.0323
	SR	0.1882	0.0499	0.0246
ISE	K	0.0019	0.0902	0.3280
	SR	0.0052	0.0677	0.1223

a random variate, the inverse transform method is simple to understand and easy to programme. Algorithm 1 shows a simplified version of the algorithm used. Note that the whole cdf of the SR is precalculated to speed up the implementation.

A Monte Carlo simulation was coded in Matlab MATLAB [30] and tested on an i7-7700HQ CPU @ 2.80 GHz (16 GB RAM), taking around 0.3 seconds to generate $N = 100000$ random variates. This low computational cost makes the approach sufficiently effective for fading channel analysis.

Two datasets were generated through Monte Carlo simulations with 100 000 samples and then compared with the analytical model. Figure 5 shows the analytical pdf for the SR distribution and the pdf simulated for both datasets. The simulated data provide a good fit with the analytic model for both datasets. The parameters used for the SR distribution were $\sigma = 0.3$ and $q = 3$ (left) and $\sigma = 6$ and $q = 5$ (right).

Table 3 shows the analytical mean and variance, in comparison with the values estimated from the Monte Carlo samples. The relative error for both measures and both cases is low (less than 2%).

This kind of simulation is only valid for mathematical analysis. To simulate the fading effects and provide the fading channel characteristics required, the modelling must be performed from the phasor formulation derived above and linked to physical variables (signal carrier frequency, signal sampling, speed of receiver, and Doppler effects). These questions are examined in the next section.

5.1. The SR Distribution for Modelling Fading Effects. The physical model is completed by reformulating the phasors

$$S = Re^{i\theta} = \sum_{i=1}^{n} A_j e^{i\Phi_j} = (X, Y) = (R\cos\theta, R\sin\theta), \quad (41)$$

as described by Rappaport [1] among others, as follows:

$$X_i(t) = \sum_{j=1}^{N} A_{ij} \cos\left(w_{ij}t - \phi_{ij}\right),$$
$$Y_i(t) = \sum_{j=1}^{N} A_{ij} \sin\left(w_{ij}t - \phi_{ij}\right). \quad (42)$$

Here, A_{ij} is the amplitude and satisfies the condition that the ensemble average $< \sum_{j=1}^{N} A_{ij}^2) >= 1$. The phase θ is now replaced by the term $\theta = w_{ij}t - \phi_{ij}$. The phase ϕ_{ij} is the random phase uniformly distributed in $[-\pi, \pi]$, $w_{ij} = \beta v \cos(\psi_{ij})$ is the Doppler shift, where v is the vehicle speed, $\beta = 2\pi/\lambda$ is the wave number, λ is the wavelength, and βv is the maximum Doppler shift (in radians per second). The angle of arrival of the signal is ψ_{ij}, also distributed in $[-\pi, \pi]$, and N is the number of sinusoidal waves, which, if large enough, ensures that both $X_i(t)$ and $Y_i(t)$ can be considered as Gaussian processes. Accordingly, the SR signal envelope is given by $r^2 = X_i^2 + Y_i^2$, and $i = 1, 2, \ldots$ The amplitude of the envelope is then fitted to the SR(σ, q) amplitude.

Taking into account the above, we first performed a Monte Carlo simulation to obtain the dataset, using 15 scattered random phasors and 20 000 samples. We then compared the resulting pdf with the analytic SR pdf. This comparison is shown in Figure 6 (left column) for two sets of SR distribution parameters ($\sigma = 2$, $q = 10$ and $\sigma = 0.3$, $q = 3$). As can be seen, the fit between the analytic and the physical models is reasonably good. Figure 6 (right column) also shows a set of simulated samples, for both cases. As can be seen, these data samples are mostly grouped around the mean value provided by the parameter setting. Note also that

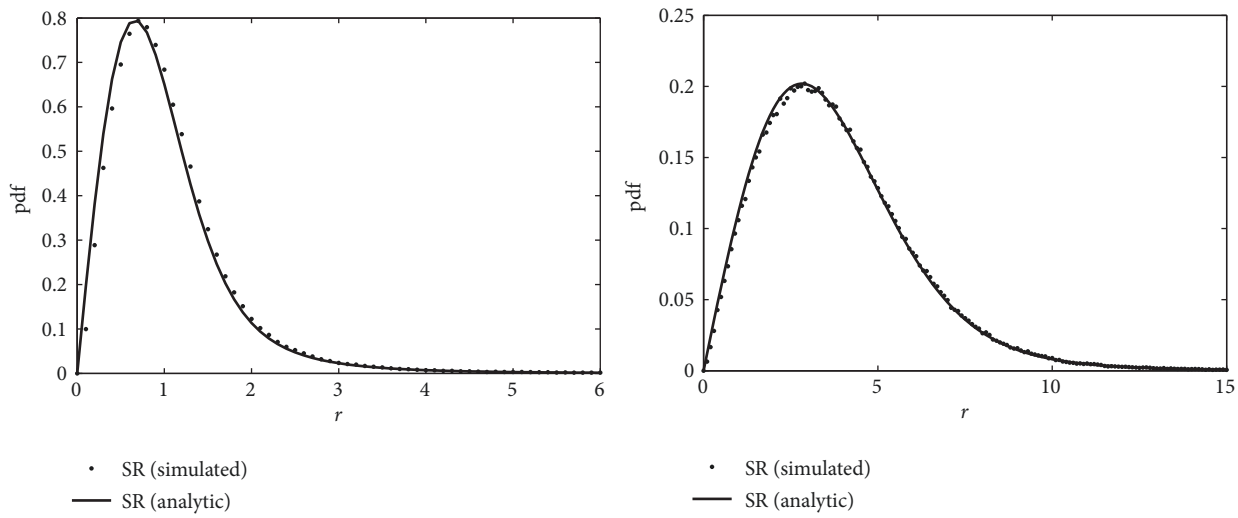

Figure 5: Comparison of the analytic SR ($\sigma = 0.3$, $q = 3$) magnitude pdf and the Monte Carlo simulated dataset (left). Comparison of the analytic SR ($\sigma = 6$, $q = 5$) magnitude pdf and the Monte Carlo simulated dataset (right).

Table 3: Comparison of the mean and variance values for the analytic SR and those estimated by statistical simulation, from the simulated data for two sets of parameters.

	SR($\sigma = 0.3$, $q = 3$)	**SR**($\sigma = 6$, $q = 5$)
Mean (analytic)	1.0297	3.8375
Mean (simulated data)	1.0491	3.8899
Relative error	1.8879%	1.3671%
Variance (analytic)	0.7397	5.2738
Variance (simulated data)	0.7360	5.2240
Relative error	0.4974%	0.9441%

Table 4: Means and variances for the analytic SR and the values estimated using phasors, from the simulated data for the two parameter sets.

	SR($\sigma = 2$, $q = 10$)	**SR**($\sigma = 0.3$, $q = 3$)
Mean (analytic)	1.9694	4.4037
Mean (simulated data)	1.9884	4.4491
Relative error	0.9662%	1.0312%
Variance (analytic)	1.1215	5.6075
Variance (simulated data)	1.0633	5.3042
Relative error	5.1908%	5.4086%

deep fading effects (– 30 dB) are present. In other words, the SR distribution correctly reflects the existence of large fading values (minimal power received at the terminal).

Table 4 shows the analytical means and variances, compared with those estimated from the Monte Carlo samples. The relative errors for both measures and both cases are low (around 5%), but larger than when the data are generated directly from the cdf, because this simulation is more complex and includes physical effects (wave scattering).

Figure 7 shows Monte Carlo simulated samples obtained using phasors for the SR ($\sigma = 0.3$, $q = 3$) and RLN ($\mu = 1.029$, $\sigma = 0.73$) distributions, with similar results (note, the RLN distribution is widely accepted for modelling fading effects).

To conclude our demonstration of how the SR distribution efficiently models fading effects, we performed a simulation of the physical channel. Algorithm 2 shows the code used. This implementation reproduces Clarke's model (mapped to the timing domain). A baseband Doppler filter was also included in the simulations, in order to generate a realistic fading spectrum, that is, to produce fading waveforms that are properly time-correlated.

Figure 8 shows a simulated fading signal for the SR ($\sigma = 0.3$, $q = 3$) distribution, corresponding to a signal with a mean value amplitude of –2.2262 dB. Five Rayleigh processes were simulated to obtain the SR(σ, q) envelope. This simulated envelope pdf of the dataset fits well with the

Input:
Alpha: α parameter ($\alpha \in \mathbb{R}$)
Q: q parameter ($q \in \mathbb{R}$)
NRays: number of emitted signals (NRays $\in \mathbb{N}$)
NRef: number of reflections (NRef $\in \mathbb{N}$)
Speed: average speed of vehicle (Speed $\in \mathbb{R}$)
Freq: carrier frequency (Freq $\in \mathbb{R}$)
FTime: simulation time (FTime $\in \mathbb{R}$)
STime: sampling time (STime $\in \mathbb{R}$)
Output:
r: signal envelope
Begin:
Power $\longleftarrow$ getPower(Alpha, Q) ▷ *Get average signal strength*
A $\longleftarrow$ $\sqrt{Alpha \cdot \text{rand}(NRays, NRef)^{-2/Q}}$ ▷ *Get signal amplitudes*
phi $\longleftarrow$ rand(NRays, NRef)$\cdot 2 \cdot \pi$ ▷ *Generate uniformly distributed phase*
psi $\longleftarrow$ rand(NRays, NRef)$\cdot 2 \cdot \pi$ ▷ *Generate uniformly distributed arriving wave*
B $\longleftarrow$ $2 \cdot \pi \cdot$ Freq$\cdot$ 3.3e-03 ▷ *Maximum Doppler frequency shift*
w $\longleftarrow\longleftarrow$ $B \cdot Speed \cdot \cos(psi)$ ▷ *Including Doppler effects*
t $\longleftarrow$ 0: STime: FTime ▷ *Time span*
x $\longleftarrow$ 0
y $\longleftarrow$ 0
for $i \longleftarrow 1$ *to NRays* **do**
  for $j \longleftarrow 1$ *to NRef* **do**
    tmp $leftarrow w \cdot t - phi$ ▷ *Get Doppler phase shift*
    $x \longleftarrow x + A \cdot \cos(tmp)$ ▷ *In-phase component*
    $y \longleftarrow y + A \cdot \sin(tmp)$ ▷ *Quadrature component*
  end for
end for
$x \longleftarrow x \cdot$ Power ▷ *Set the average signal strength*
$y \longleftarrow y \cdot$ Power ▷ *Set the average signal strength*
$r \longleftarrow \sqrt{x^2 + y^2}$ ▷ *Calculate the signal envelope*
End

Algorithm 2: Fading simulation.

analytical one (not shown). In this case, the envelope includes very deep fading levels (around −40 dB) which, although rather infrequent have been reported in rapid fading in long-distance HF propagation (see M et al. [31]). The results shown are for two vehicle velocities (60 km/h and 120 km/h). The Doppler effect is significantly more apparent at the higher velocity, as expected.

In the present paper, the physical interpretation of the parameters of the SR distribution is not discussed, but it seems clear from expression (13), and Algorithm 2, that there must exist a straightforward relation between these two parameters and the average signal power strength (through the means and variances for the amplitude of scattered waves). However, more analysis of this question is needed for a complete physical interpretation.

A simulator block implementing the SR(σ, q) signal has been developed (coded in Matlab) and included in a more general mobile radio channel software simulator, which performs Gaussian/uniform processes to simulate the phasors and thus obtain the signal envelope distributed with SR(σ, q) pdf. Some typical routines are also included, such as a n-pole Tchebicheff filter block and a simple RF combiner (for the equal gain and maximum-ratio cases), together with the possibility of simulating samples for the other commonly used fading distributions (i.e., Rayleigh, GR and RLN).

6. Final Comments

In this paper, we present a new distribution, the two-parameter SR distribution, which is competitive with the RLN distribution and the K distribution. The Rayleigh distribution is considered as a special case when one of the parameters tends to infinity. Parameter estimation for the new distribution is also discussed. From a mathematical standpoint, the distribution we propose has certain advantages over the RLN distribution within the framework of fading signal strength. Two methods to obtain the simulated envelope are discussed; the first is based strictly on the pdf of the distribution, and the second is based on a physical model constructed from the Rayleigh physical model, using the classical method described by Clarke. In addition, closed-form expressions are derived for the average channel capacity and the bit error rate (BER) for DPSK and MSK modulations for the proposed distribution.

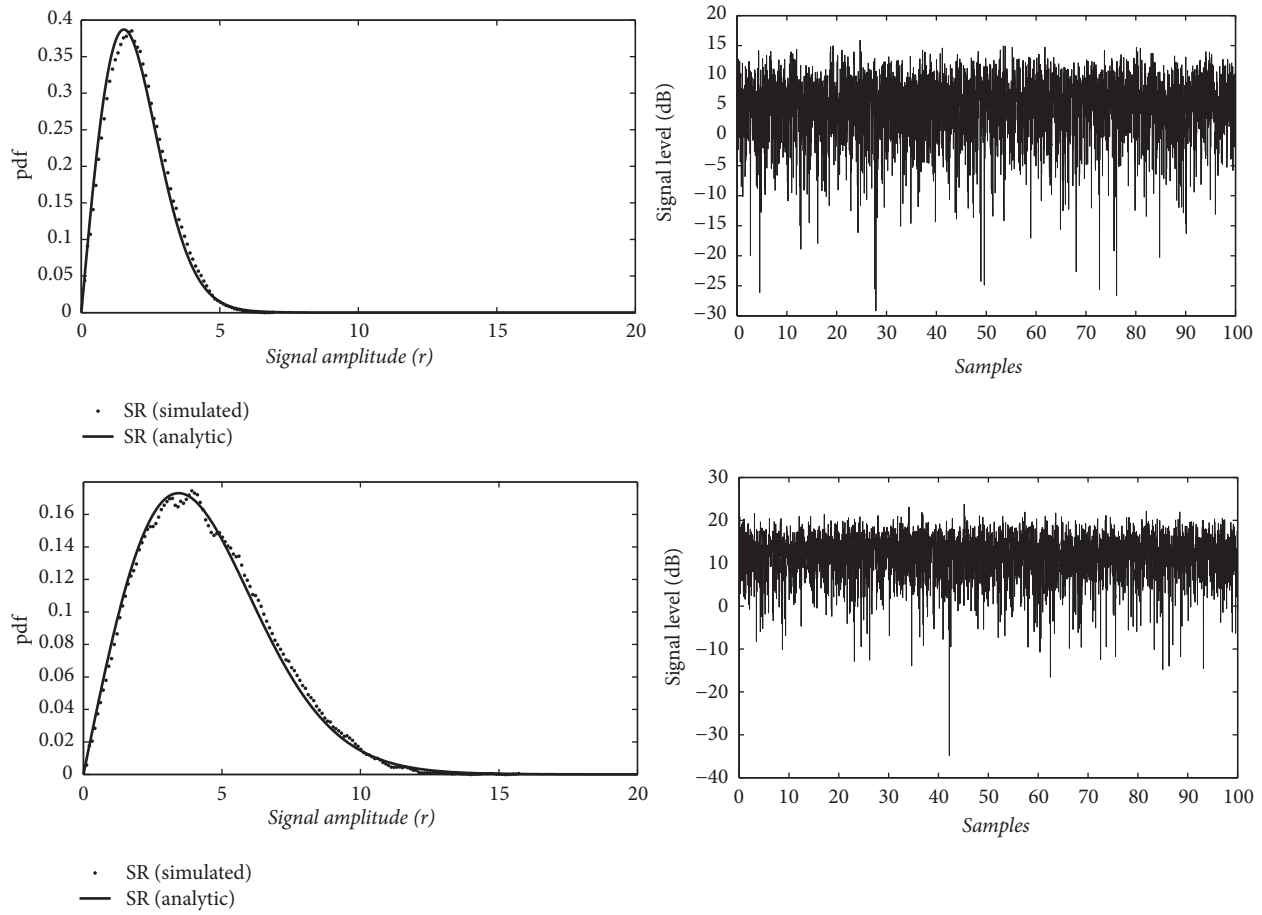

Figure 6: Samples simulated by using phasors of the SR distribution ($\sigma = 2$, $q = 10$) (top, left) and a set of simulated samples (top, right). Samples simulated by using phasors of the SR distribution ($\sigma = 0.3$, $q = 3$) (bottom, left) and a set of simulated samples (bottom, right). For both cases, the analytic SR distribution is also shown, for the sake of comparison.

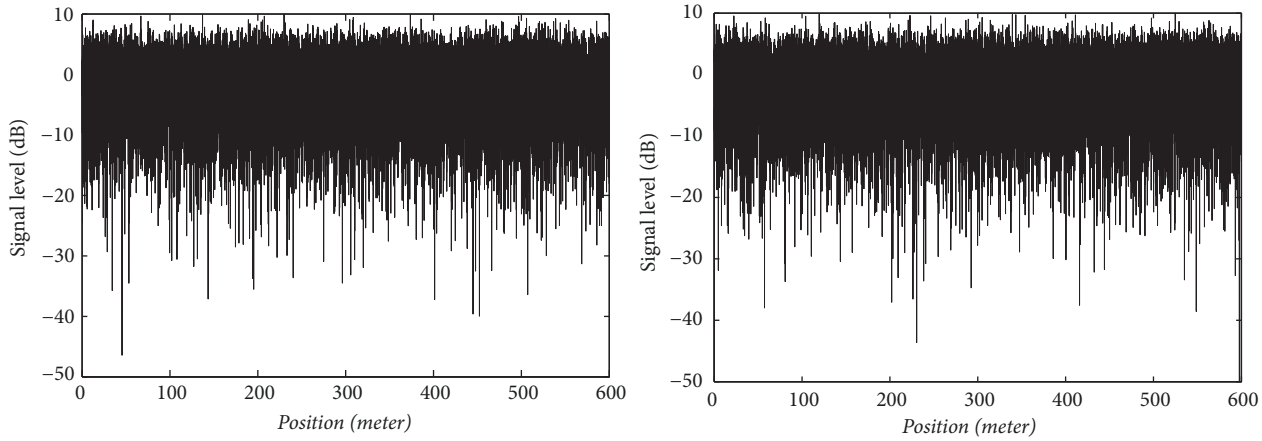

Figure 7: Simulated samples of the RLN distribution ($\mu = 1.029$, $\sigma = 0.73$) (left). Simulated samples of the SR distribution ($\sigma = 0.3$, $q = 3$) (right). The parameters used in both cases are those providing same mean and standard deviation values and are represented spaced 0.1 wavelength apart for the 0 dB mean value.

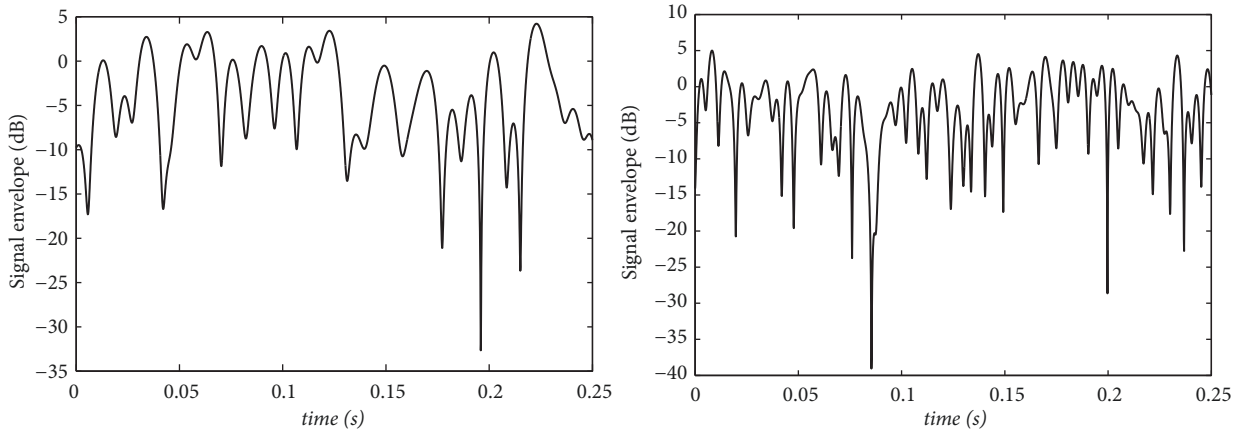

FIGURE 8: Fading signal for the SR distribution ($\sigma = 0.3$, $q = 3$); carrier frequency = 900 MHz and speed = 60 Km/h (left) and speed = 120 km/h (right).

Data Availability

The data used to support the findings of this work can be reproduced by referring to the mathematical formulas and the algorithms described. In addition, the codes used are available from the corresponding author upon request. These data include Mathematica and Matlab codes and therefore users will require the corresponding licenses.

Conflicts of Interest

The authors declare that they have no conflicts of interest.

Acknowledgments

E. Gómez-Déniz was partially funded by Grant ECO2013-47092, Ministerio de Economía y Competitividad, Spain, and ECO2017-85577-P, Ministerio de Economía, Industria y Competitividad, Agencia Estatal de Investigación. The research of H. W. Gómez was supported by MINEDUC-UA project, Code ANT 1755.

References

[1] T. S. Rappaport, *Wireless Communications: Principles and Practice*, Prentice Hall Communications Engineering and Emerging Technologies Series, 2nd edition, 2001.

[2] R. M. Barts and W. L. Stutzman, "Modeling and simulation of mobile satellite propagation," *IEEE Transactions on Antennas and Propagation*, vol. 40, no. 4, pp. 375–382, 1992.

[3] A. Borhani, G. L. Stuber, and M. Patzold, "A random trajectory approach for the development of nonstationary channel models capturing different scales of fading," *IEEE Transactions on Vehicular Technology*, vol. 66, no. 1, pp. 2–14, 2017.

[4] J. Lopez-Fernandez, J. F. Paris, and E. Martos-Naya, "Bivariate rician shadowed fading model," *IEEE Transactions on Vehicular Technology*, vol. 67, no. 1, pp. 378–384, 2018.

[5] S. Suh, *A Propagation Simulator for Land Mobile Satellite*, Virginia Tech, 1998.

[6] F. Hansen and F. I. Meno, "Mobile fading Rayleigh and lognormal superimposed," *IEEE Transactions on Vehicular Technology*, vol. 26, no. 4, pp. 332–335, 1977.

[7] A. Abdi and M. Kaveh, "K distribution: an appropriate substitute for Rayleigh-lognormal distribution in fading-shadowing wireless channels," *IEEE Electronics Letters*, vol. 34, no. 9, pp. 851-852, 1998.

[8] J. Proackis and M. Salehi, *Digital Communications*, McGraw-Hill Education, 2007.

[9] F. Adachi, M. T. Feeney, and J. D. Parson, "Level crossing rate and average fade duration for time diversity reception in Rayleigh fading conditions," *IEE Proceedings F - Communications, Radar and Signal Processing*, vol. 135, no. 6, pp. 501–506, 1988.

[10] P. Subbarayan, "Minimum shift keying: A spectrally efficient modulation," *IEEE Communications Magazine*, vol. 17, no. 4, pp. 14–22, 1979.

[11] Y. A. Iriarte, H. W. Gómez, H. Varela, and H. Bolfarine, "Slashed Rayleigh distribution," *Revista Colombiana de Estadística*, vol. 38, no. 1, pp. 31–44, 2015.

[12] D. Tse, *Fundamentals of Wireless Communication*, University Press, Cambridge, UK, 2005.

[13] G. Stuber, *Principles of Mobile Communication*, Kluwer, Boston, Mass, USA, 1996.

[14] H. Ruskeepaa, *Mathematica Navigator. Mathematics, Statistics, and Graphics*, Academic Press, USA, 3rd edition, 2009.

[15] Karmeshu and R. Agrawal, "On efficacy of Rayleigh-inverse Gaussian distribution over K-distribution for wireless fading channels," *Wireless Communications and Mobile Computing*, vol. 7, no. 1, pp. 1–7, 2007.

[16] E. Gómez-Déniz and L. Gómez-Déniz, "A generalisation of the Rayleigh distribution with applications in wireless fading channels," *Wireless Communications and Mobile Computing*, vol. 13, no. 1, pp. 85–94, 2016.

[17] M. D. Yacoub, J. E. V. Bautista, and L. Guerra de Rezende Guedes, "On higher order statistics of the Nakagami-m distribution," *IEEE Transactions on Vehicular Technology*, vol. 48, no. 3, pp. 790–794, 1999.

[18] P. Beckmann, *Probability in Communication Engineering*, Harcourt, Brace & World, New York, NY, USA, 1967.

[19] A. Goldsmith, *Wireless Communications*, Cambridge University Press, 2005.

[20] S. K. Bhattacharya, "Confluent hypergeometric distributions of discrete and continuous type with applications to accident proneness," *Calcutta Statistical Association Bulletin*, vol. 15, pp. 20–31, 1966.

[21] A. Abdi and M. Kaveh, "Comparison of DPSK and MSK bit error rates for K and rayleigh-lognormal fading distributions," *IEEE Communications Letters*, vol. 4, no. 4, pp. 122–124, 2000.

[22] J. Li, A. Bose, and Y. Zhao, "Rayleigh flat fading channels' capacity," in *Proceedings of the 3rd Annual Communication Networks and Services Research Conference (CNSR'05)*, pp. 1–8, 2005.

[23] R. Singh and M. Rawat, "Closed-form distribution and analysis of a combined nakagami-lognormal shadowing and unshadowing fading channel," *Journal of Telecommunications and Information Technology*, no. 4, pp. 81–87, 2015.

[24] W. Gautschi, F. E. Harris, and N. M. Temme, "Expansions of the exponential integral in incomplete gamma functions," *Applied Mathematics Letters*, vol. 16, no. 7, pp. 1095–1099, 2003.

[25] S.-D. Lin, Y.-S. Chao, and H. M. Srivastava, "Some expansions of the exponential integral in series of the incomplete gamma function," *Applied Mathematics Letters*, vol. 18, no. 5, pp. 513–520, 2005.

[26] D. Cygan, "Analytical evaluation of average bit error rate for the land mobile satellite channel," *International Journal of Satellite Communications and Networking*, vol. 7, no. 2, pp. 99–102, 1989.

[27] P. Hall, "On Kullback-Leibler loss and density estimation," *The Annals of Statistics*, vol. 15, no. 4, pp. 1491–1519, 1987.

[28] J. Lin, "Divergence measures based on the Shannon entropy," *IEEE Transactions on Information Theory*, vol. 37, no. 1, pp. 145–151, 1991.

[29] A. W. Bowman, "An alternative method of cross-validation for the smoothing of density estimates," *Biometrika*, vol. 71, no. 2, pp. 353–360, 1984.

[30] MATLAB, "The MathWorks Inc.," Natick, Mass, USA, 2015.

[31] M. D. Yacoub, J. E. V. Bautista, and L. G. D. R. Guedes, "On higher order statistics of the Nakagami-m distribution," *IEEE Transactions on Vehicular Technology*, vol. 48, no. 3, pp. 790–794, 1999.